Ecological Applications, 24(6), 2014, pp. 1289–1296

Mapping tropical forest canopy diversity using high-fidelity imaging spectroscopy

Jean-Baptiste Féret[1] and Gregory P. Asner

Department of Global Ecology, Carnegie Institution for Science, 260 Panama Street, Stanford, California 94305 USA

Abstract. There is a growing need for operational biodiversity mapping methods to quantify and to assess the impact of climate change, habitat alteration, and human activity on ecosystem composition and function. Here, we present an original method for the estimation of α- and β-diversity of tropical forests based on high-fidelity imaging spectroscopy. We acquired imagery over high-diversity Amazonian tropical forest landscapes in Peru with the Carnegie Airborne Observatory and developed an unsupervised method to estimate the Shannon index (H') and variations in species composition using Bray-Curtis dissimilarity (BC) and nonmetric multidimensional scaling (NMDS). An extensive field plot network was used for the validation of remotely sensed α- and β-diversity. Airborne maps of H' were highly correlated with field α-diversity estimates ($r = 0.86$), and BC was estimated with demonstrable accuracy ($r = 0.61$–0.76). Our findings are the first direct and spatially explicit remotely sensed estimates of α- and β-diversity of humid tropical forests, paving the way for new applications using airborne and space-based imaging spectroscopy.

Key words: alpha diversity; Amazon basin; beta diversity; Bray-Curtis dissimilarity; canopy diversity; Carnegie Airborne Observatory; hyperspectral remote sensing; Shannon index; spectral species distribution.

Introduction

Tropical forests harbor the highest density of canopy plant species on Earth, yet we have little knowledge of environmental controls on local-scale tropical forest diversity, referred to as α-diversity (Whittaker 1960). We have even less information on patterns of community compositional variations (β-diversity) throughout tropical landscapes. Mapping α- and β-diversity would greatly expand our understanding of tropical forest composition and change.

Remote sensing offers to bridge a spatial divide between field plots and our understanding of possible environmental controls on tropical forest diversity patterns. Satellite studies have indirectly related canopy brightness, topography, and other remotely sensed habitat indicators to species richness and community composition (e.g., Rajaniemi et al. 2005). Yet no studies have made a direct link between the spectral reflectance signature variation of canopies and either α- or β-diversity in tropical forests. Recent reviews suggest that species detection is maturing as a remote sensing science (Gillespie et al. 2008), and imaging spectroscopy (hyperspectral remote sensing) has emerged as a leading technology for biodiversity mapping (Asner 2013). With contiguous spectral sampling over broad optical wavelength regions, imaging spectroscopy has begun to produce locational estimates of particular species and/or assemblages of species (e.g., Clark et al. 2005). Despite this progress, general and robust biodiversity detection methods are needed to map α- and β-diversity in very speciose ecosystems such as tropical forests. Here we present a new unsupervised algorithm to map of α- and β-diversity using high-fidelity airborne imaging spectroscopy. After developing the theoretical basis for the algorithm, we test it on lowland tropical forests of the Amazon basin using an extensive field plot network.

Manuscript received 27 September 2013; revised 18 December 2013; accepted 23 December 2013. Corresponding Editor: D. Schimel.

[1] E-mail: feretjb@cesbio.cnes.net

Materials and Methods

Study sites

Several validation areas were selected in the Peruvian Amazon, which cover a wide range of elevation, floristic, and edaphic conditions. The areas included southern lowland, high-fertility forests (Centro de Investigación y Capacitación Rio Los Amigos, or CICRA), northern lowland forests characterized by dystrophic white sands (Allpahuayo), submontane forests of 400–900 m in elevation (Quincemil), and montane forests from 1500 m to treeline at 3700 m (Kosñipata; Asner et al. 2013). These landscapes encompass a portion of the Carnegie spectranomics field plot network described in *Materials and Methods: Field plots* and in Appendix A.

Airborne data

We used the Carnegie Airborne Observatory (CAO) airborne taxonomic mapping system (AToMS) to map the study landscapes in July–August 2011. CAO AToMS integrates a visible-to-shortwave infrared (VSWIR) imaging spectrometer with a waveform light detection and ranging (LiDAR) scanner (Asner et al.

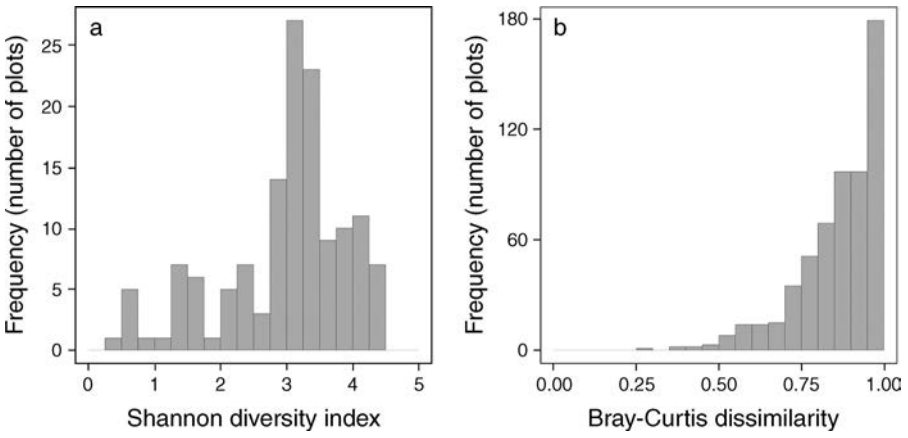

FIG. 1. Distribution of (a) the Shannon index (α-diversity) and (b) Bray-Curtis dissimilarity (β-diversity) measured at the genus level and derived from the Carnegie biodiversity plot network throughout western Amazonia.

2012). The VSWIR spectrometer measures spectroscopic radiance in 5-nm increments across a 380–2510 nm wavelength range. These measurements were resampled to 10-nm, full-width at half-maximum resolution, resulting in 214 contiguous spectral bands covering the entire wavelength range. Our flying altitude of 2000 m resulted in 2-m spatial resolution. The spectroscopic images were ortho-georectified, and then calibrated to apparent surface reflectance using the ACORN5-LiBatch atmospheric correction model, which is based on MODTRAN-4 (Imspec, Pasadena, California, USA). After eliminating spectral channels affected by atmospheric water absorption, 164 high-quality bands were retained. The LiDAR data were used to mask ground and shade, and a minimum normalized difference vegetation index (NDVI) of 0.5 was used to remove non-foliar pixels (Asner and Martin 2009).

Field plots

Field data collection was aimed at producing a plot network for the validation of both α- and β-diversity mapping methods. Each field plot located in one of the four aforementioned study areas was semicircular in shape and 0.14 ha in size (~350 CAO VSWIR pixels), and the plot boundaries were geolocated using a global positioning system (GPS) with differential correction (Leica GS50, Leica Geosystems, Heerbrugg, Switzerland). In each plot, all trees and lianas with diameter at breast height (defined as 130 cm above ground) $\geq$10 cm were identified to species. A voucher was collected, which was later identified at the Peruvian National Herbarium at La Molina, the Missouri Botanical Garden, or the Carnegie Spectranomics Library (Stanford, California, USA). Validation of remotely sensed α-diversity was accomplished using 153 CAO-to-field plot combinations. Validation of β-diversity was performed using 91 plot pairs from CICRA (14 individual plots) and 496 plot pairs from Allpahuayo (32 individual plots). More information about the field data collection is given in Appendix A. Additionally, Fig. 1 provides the distribution of the two biodiversity indices (Shannon diversity index and Bray-Curtis dissimilarity) used to estimate α- and β-diversity.

Plot simulations

In addition to the biodiversity plots inventoried in the field, individual tree crowns at CICRA corresponding to 36 species were identified and geolocated with a GPS. For each species, 200–2000 pixels corresponding to at least two crowns were extracted from the mosaic, for a total number of about 16 000 sunlit pixels. These data were used to simulate a large number of plots of variable species richness. Each simulated plot was defined by a square surface of 36×36 pixels (0.52 ha). Nine richness levels were simulated corresponding to 1, 2, 3, 4, 6, 9, 12, 18, and 36 species equally abundant in the plot. For each richness level, 36 plots were simulated, each corresponding to a unique combination of species. Pixels corresponding to each species were randomly selected, avoiding repeat combinations. These simulated plots were arranged along a modeled diversity gradient (Fig. 2), which was used to develop and fine-tune a new method aimed at the estimation of canopy biodiversity. The purpose of our method is primarily to map non-directional variations of species composition over the landscape, so we will not focus on metrics specific to study of species turnover along a directional gradient (Anderson et al. 2011).

Biodiversity indices

We estimated α-diversity for our field plot network using the Shannon index H' (Shannon 1948):

$$H' = -\sum_{i=1}^{n} p_i \times \log(p_i). \quad (1)$$

Here p_i represents the relative proportion of individuals

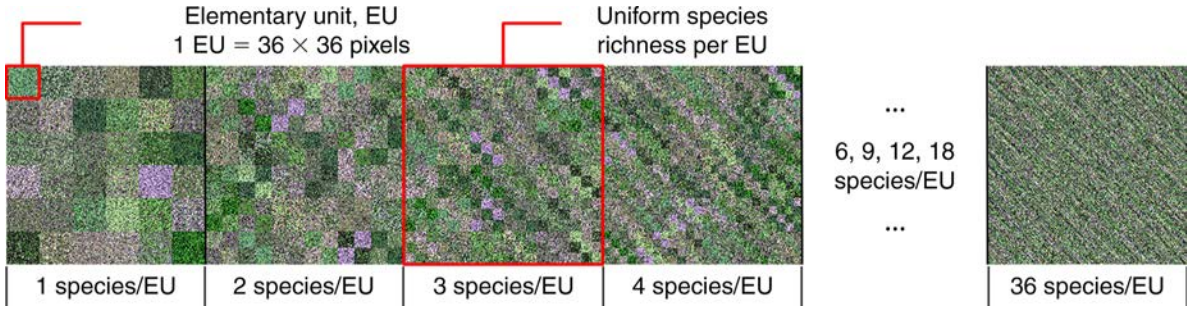

FIG. 2. Red-green-blue (RGB) image composites of a simulated gradient of increasing α-diversity. Each pixel of this simulated gradient corresponds to a pixel extracted from an actual Carnegie Airborne Observatory (CAO) image in which tree crowns were identified in the field. The color contrast between species is real and due to rescaling of the RGB channels. For each of the 36 species used to create this diversity gradient, at least two tree crowns were used in order to include spectral variability of individuals in the same species.

of species i, and n represents the total number of species in the plot. β-diversity was computed using the pairwise Bray-Curtis (BC) dissimilarity index (Bray and Curtis 1957):

$$\mathrm{BC}_{ij} = \frac{\sum_{s=1}^{n} |x_{is} - x_{js}|}{\sum_{s=1}^{n} (x_{is} + x_{js})} \quad (2)$$

where BC_{ij} is the dissimilarity between plots i and j, and x_{is} and x_{js} are the abundances of species s in plots i and j, respectively. BC ranges from 0 to 1, where 0 indicates two sites with identical species composition, and 1 indicates two sites sharing no species. BC is an estimate of the overlap between species distributions corresponding to the proportion of co-occurring individuals among the total number of individuals contained in different plots (Bloom 1981).

These definitions apply to species, as well as higher taxonomic levels such as genus or family. In our study, H' measured at the species level was highly correlated with genus-level results ($r = 0.99$; $P < 0.001$), with H' values ranging from 0.33 to 4.86 at the species level, and from 0.33 to 4.36 at the genus level. The correlation between BC estimated at species and genus levels was also high ($r = 0.86$; $P < 0.001$). This indicated that estimations of H' and BC at the species and genus levels are equivalent in our sites. We chose to work at the genus level as the distribution of measured BC spanned over a broader range of variation than did the distribution measured at the species level.

Spectral diversity metrics

Our method for estimating canopy diversity builds off previous work based on the spectral variation hypothesis (Palmer et al. 2002), which was developed to assess spectral heterogeneity induced by variations in habitat. This assertion is justified when working with medium-to-low spatial resolution data, as the spectral information contained in each pixel represents the integrated spectral properties of different species. However, work with fine spatial resolution images highlights the strong taxonomic signal often encountered in humid tropical forest canopies (e.g., Clark et al. 2005), allowing us to consider spectral variation as a direct estimate for canopy diversity. Nonetheless, some species are spectrally too similar to be discriminated, while other species are easily differentiable. Existing methods relating biodiversity to metrics such as variations in NDVI (sNDVI) or the mean distance from spectral centroid (MDC) usually compute spectral heterogeneity at the local scale (Appendix D), and do not take into account the global distribution in spectral space. Fig. 3 is a schematic illustration of the distribution of the pixels measured in two plots (spatial units) of identical spatial dimension in a two-dimensional spectral space: the first plot (Fig. 3a) includes two species occupying distant locations in the spectral space, and the second plot (Fig. 3b) includes five species spectrally separable but grouped in a compact portion of this spectral space. The dotted line indicates the contour of the spectral space corresponding to the total landscape. In this illustration, the spatial unit represented in Fig. 3a contains the lowest biodiversity but has the highest MDC. Although extreme, this example illustrates the risk of using a one-dimensional metric such as MDC to describe the variability in the spectral space for high spatial resolution data. To overcome this challenge, we propose a new approach based on segmentation of the spectral space defined by the airborne data acquired across the landscape. This is based on the hypothesis that species are often spectrally separable from one another, occupying a spectral subspace of limited size defined by their chemical and structural properties within a community (Asner and Martin 2009).

Our approach assumes that the spectral space corresponding to a landscape is a combination of subspaces, each of them related to one or several species sharing similar spectral signatures. Each of these subspaces can be referred to as a "spectral species," as it includes only a limited number of the numerous species existing across landscapes. Our approach does not attempt to directly relate spectral

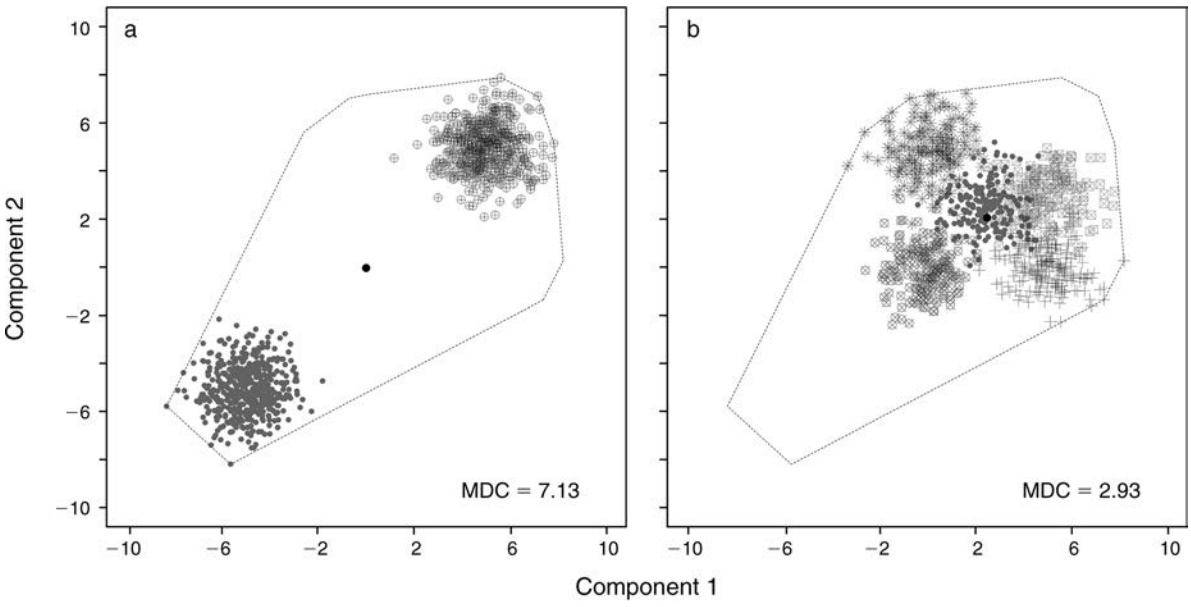

FIG. 3. Simulation of (a) one plot containing two species distant from one another in spectral space and (b) one plot containing five species spectrally separable but close to one another in spectral space. The black dot locates the centroid, and the mean distance from spectral centroid (MDC) is calculated for each plot. The dotted gray line indicates the limits of the spectral space defined by the two plots. The term "Components" used in this figure may correspond to spectral components in the original spectral space (spectral band) or components in a transformed space (i.e., components obtained after the application of the principal component analysis to the data). The units used here are arbitrary units.

species to biological species observed on the ground, but the spectral species distribution (SSD) we derive for an area approximates the diversity of species observed in the field (Asner and Martin 2011). Spectral species are defined using an unsupervised approach based on the clustering of a random subset collected across the landscape. Once a set of spectral species is defined, each pixel contained in a plot is assigned to one of these spectral species. A key property of our method is that we can process spectral species as a replacement for actual species, making possible not only the estimation of local diversity, but also dissimilarity between communities across a landscape. However, the number of spectral species to be defined has to be consistent between landscapes in order to allow identical range of variation for α-diversity. To estimate α- and β-diversity, our mapping method is described in six steps (Fig. 4 and Appendices). (1) A continuum removal (CR) transformation is applied to the spectral data. This suppresses the overall brightness variation (albedo) among spectra, thereby minimizing effects of changing illumination conditions between flight lines. (2) Principal component analysis (PCA) is applied to the CR spectral data followed by a principal component (PC) selection to decrease spectral dimensionality. (3) A subset of pixels is randomly selected across the entire mapped landscape, and the spectral space containing this subset is partitioned into spectral species using k-means clustering ($k = 40$, 20 random starts), and their centroid is located. (4) The spectral data set is divided into final mapping units (here, images are divided into 1-ha kernels for α-diversity and 4-ha kernels for β-diversity). Within each mapping unit, each image pixel is assigned to a given spectral species, with a maximum of 40 spectral species per kernel (or "digital plot"), based on the minimal Euclidean distance between the pixel and the previously defined centroids. The number of spectral species was chosen based on sensitivity analysis performed with the simulated biodiversity data to optimize the estimation of H'. (5) A spectral species distribution is obtained for each mapping unit. The Shannon index (α-diversity) and the pairwise Bray-Curtis dissimilarity (β-diversity) are computed from this distribution. (6) To decrease the risk of non-representative random sampling, steps 4 and 5 are repeated 100 times, and the metrics estimated for each mapping unit are averaged. All analyses are performed using R 2.14.2 with "hyperSpec" (Beleites and Sergo 2012). A pseudo-code of the method is provided in Appendix B.

We compared two methods of PC selection. First, we selected the number of PCs necessary to reach 99% of total variance explained in the image. We also selected PCs based on visual analysis, focusing on the components revealing patterns likely to be related to biological diversity, and discarding components driven by variation in illumination, sensor noise, and other artifacts (Appendix C). We also quantitatively compared the performance of the SSD approach to the sNDVI and MDC (Appendix D).

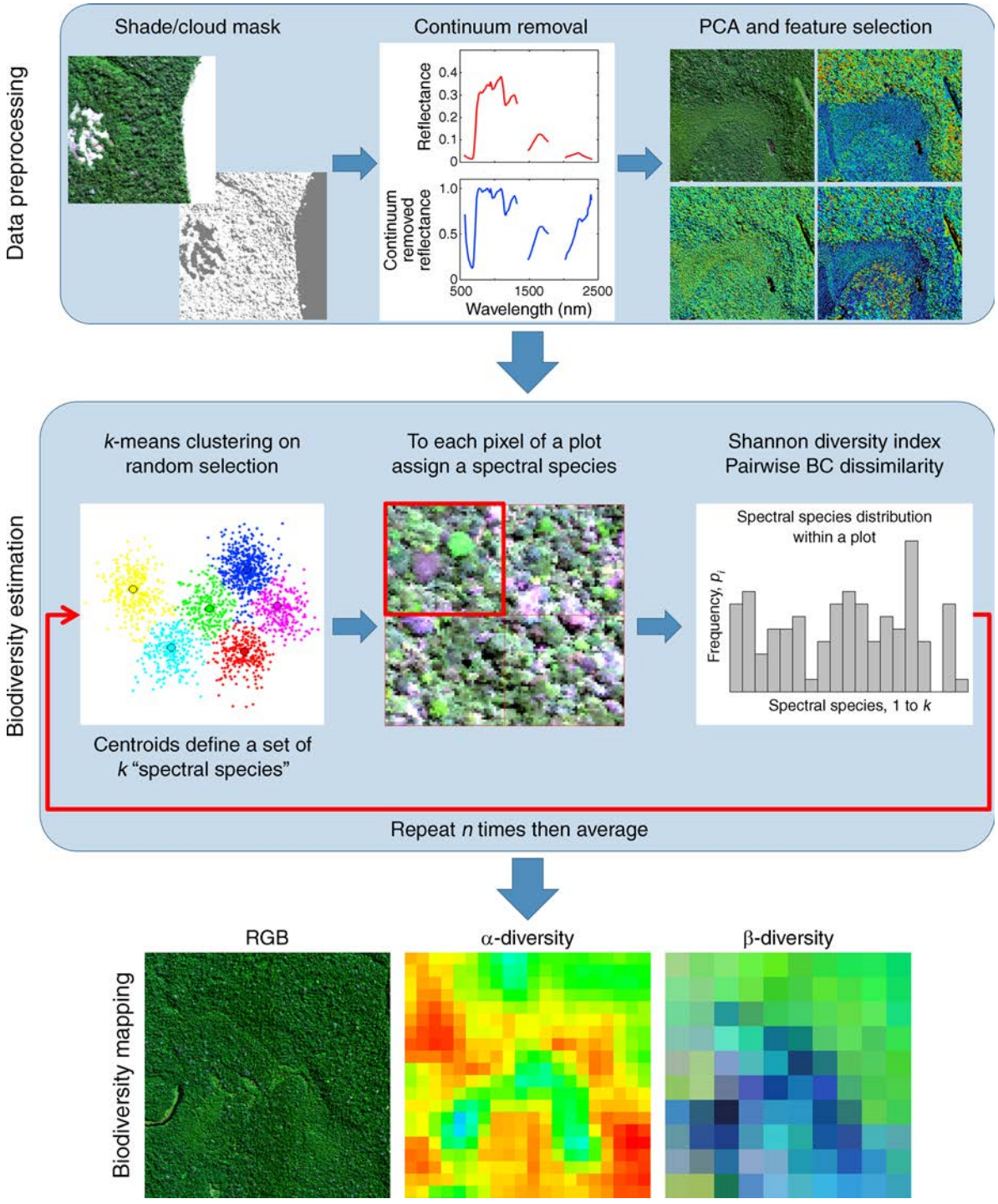

FIG. 4. Diagrammatic representation of the steps for estimating α-diversity at 1-ha resolution and β-diversity at 4-ha resolution. PCA stands for principal component analysis.

RESULTS AND DISCUSSION

Validation of the estimation of biodiversity

Comparison of the different methods used to remotely estimate H' (sNDVI, MDC, SSD) indicated that SSD strongly outperformed the others, on both the simulated diversity gradient and the actual biodiversity plot network (Table 1). The sNDVI showed very low performance in estimating H' (particularly when applied to the field plots), which can be explained by the

TABLE 1. Pearson's correlation coefficient between H' (measured from both simulated diversity gradient and diversity plot network) and corresponding remotely sensed H' estimated using different methods.

	Simulated diversity		Field diversity plots	
Method	Visual	Variance (%)	Visual	Variance (%)
sNDVI	0.15**		0.06	
MDC	0.38**	0.39**	0.26*	0.31*
SSD	0.91**	0.90**	0.86**	0.73**

Notes: For the mean distance from spectral centroid (MDC) and spectral species distribution (SSD) approaches, two strategies for principal component (PC) selection are compared, based either on the visual interpretation or on the total percentage of variance explained by the PCs (see Appendix C). Note that because sNDVI is not based on PCs, only one value is given for this method.

* $P < 0.05$; ** $P < 0.001$.

relatively low degree of information content in the two spectral bands used to compute the NDVI. In comparison, MDC was slightly more successful than was the sNDVI for both simulated and field diversity plots; however, the correlation with measured H' remained weak.

Remote estimation of H' always performed better on the simulated diversity plots than on the actual field plots (Table 1). The simulated plots were of lower species richness, with a maximum of 36 species, and each crown occupied the same amount of lateral space. In contrast, the actual trees and lianas inventoried in the field plots varied widely in structure and spatial occupancy. Nonetheless, the simulations provided information on the sensitivity of the method to the number of spectral species. One result not appearing in Table 1 was the bias of the estimated H', which lead to systematic underestimation. This is explained by the purposefully limited number of spectral species (40) compared to the maximum taxonomic diversity inventoried in the plots, but it can be easily corrected with a linear factor derived from the relationship obtained between field data and estimation. We systematically applied this correcting factor to all absolute H' values reported in our study (including maps). A key difference between the results obtained with simulated plots and actual field plots was most apparent in terms of the strategy for PC selection (Appendix C). The choice of total-variance or visual selection of PCs did not influence the estimation of H' in the simulated biodiversity plots due to the lack of spatial structure and the use of vegetated sunlit pixels, which is not the case with airborne imagery, despite our efforts to filter data. There was a noticeable influence of PC selection on the estimation of H' for the actual field plots: the Pearson correlation obtained after visual selection of PC reached 0.86 ($P < 0.001$), whereas it was limited to 0.73 ($P < 0.001$) when selecting PCs based on total variance. We conclude here that H' estimation based on the SSD approach with visual PC selection is more accurate. The resulting regression yielded an RMSE of 0.55 in H' units (after linear correction based on validation) over a range of nearly five H' units (Fig. 5a). Given the skewed distribution of H', the Kendall tau rank correlation coefficient was also calculated to confirm the correlation ($\tau = 0.61$, $P < 0.001$). We also computed the Pearson correlation between the measured H' and the H' estimated for each of the 100 iterations. The mean value was 0.83 (range, 0.80–0.86). This result is analogous to signal averaging, which consists in increasing signal-to-noise ratio by replicating measurements, and confirms that the iterative construction of our method optimizes the estimated Shannon index. Mantel correlation was also computed between the BC matrix obtained from plot inventory and remote sensing (Fig. 5b), indicating significant correlation for Amazonian field validation sites ($r_M = 0.75$ at CICRA, $r_M = 0.61$ at Allpahuayo, $P <$

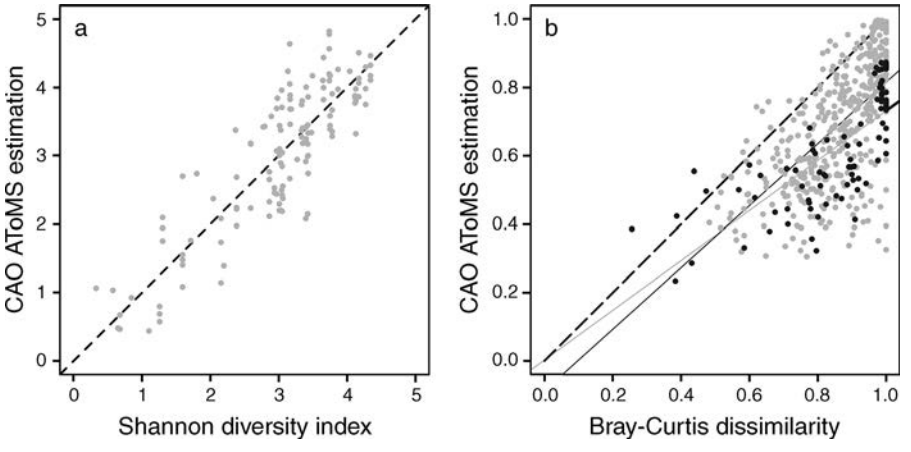

FIG. 5. Validation of (a) remotely sensed Shannon index for α-diversity (a linear correcting factor was applied to eliminate bias) and (b) Bray-Curtis dissimilarity for β-diversity. In panel (b), plots from the Centro de Investigación y Capacitación Rio Los Amigos (CICRA) and Allpahuayo landscapes, respectively, are black and gray dots with corresponding black and gray solid regression lines. In both panels, the dashed line represents 1:1. AToMS stands for the airborne taxonomic mapping system of the Carnegie Airborne Observatory (CAO).

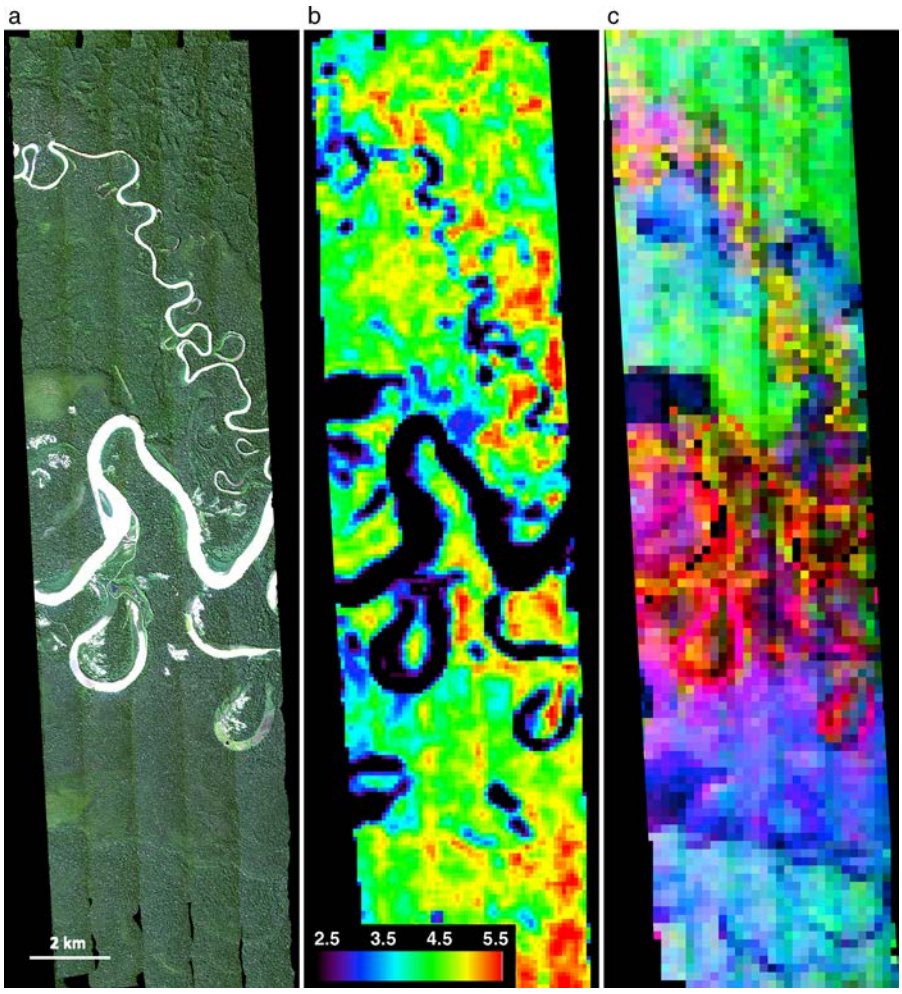

FIG. 6. Example of biodiversity mapping results throughout the CICRA landscape in lowland Amazonia. Panels are as follows: (a) natural color composite image from the CAO visible-to-shortwave infrared (VSWIR) imaging spectrometer; (b) α-diversity based on the Shannon index; and (c) β-diversity based on Bray-Curtis dissimilarity (no color scale is applicable, and a larger Bray-Curtis dissimilarity between two plots corresponds to larger differences in color in the RGB space between the two corresponding pixels).

0.001). The estimated BC was systematically underestimated for the same reasons as explained for H'; however, we did not perform any correction in order to keep BC between 0 and 1.

Additional study is required to better understand which spectral domains contribute the most to the selected PCs in order to better describe the key physical and chemical factors leading to an accurate estimation of biodiversity. This knowledge will contribute to the development of a fully automated diversity mapping method in the future.

Based on our results, α- and β-diversity were mapped throughout the Amazonian landscapes using the SSD approach. One example image set is shown in Fig. 6 for the CICRA landscape. For β-diversity, we added nonmetric multidimensional scaling (NMDS) to project samples in three-dimensional Euclidean space while preserving the rank-order of the Bray-Curtis dissimilarity matrix (Baldeck and Asner 2013). The map displays similar species composition with similar colors, and different species composition with changes in color. We did not attempt to interpret each of these three dimensions in terms of species composition, as they vary from one site to the next, and our diversity plot network did not cover all communities. However, more field observations and inventories could help in interpreting the different colors in terms of species composition.

Methodological limitations

The total diversity within a spectroscopic image taken over a tropical forest may bias the mapped biodiversity and complicate inter-sites comparisons. For our method, "spectral species" are defined by the segmentation of the spectral space, and the maximum potential number of spectral species is selected, or fixed, from one

landscape to another. As a consequence, besides the negative bias observed when studying highly diverse ecosystems, the biodiversity estimated across a site harboring low taxonomic diversity and a compact spectral space may show a similar range of variation as one estimated for a site harboring high biological diversity and a much more extended spectral space, thereby leading to a relative overestimate of the former compared to the latter. However, our results suggest that values of α-diversity obtained from images of different Amazonian forests do not require adjustments before inter-site comparison. Despite current limitations, our findings highlight the potential of imaging spectroscopy to map canopy diversity throughout compositionally complex ecosystems, and they pave the way for additional mapping studies of tropical canopy diversity at fine spatial scales.

Implications for ecological applications

Knowledge of biodiversity distributions is currently sparse worldwide, and existing information is usually collected locally but on very coarse geographic scales compared to global environmental data. This knowledge gap makes it difficult to understand the interactions between biodiversity and nearly every other ecological/environmental driver (Kreft and Jetz 2007). The possibility of estimating biodiversity and species compositional variations at fine geographic scales may reduce this knowledge gap to allow increased understanding of biodiversity responses to global change.

Acknowledgments

The Carnegie Airborne Observatory is made possible by the Avatar Alliance Foundation, Grantham Foundation for the Protection of the Environment, Gordon and Betty Moore Foundation, the John D. and Catherine T. MacArthur Foundation, W. M. Keck Foundation, the Margaret A. Cargill Foundation, Mary Anne Nyburg Baker and G. Leonard Baker, Jr., and William R. Hearst III.

Literature Cited

Anderson, M. J. et al. 2011. Navigating the multiple meanings of β diversity: a roadmap for the practicing ecologist. Ecology Letters 14:19–28.

Asner, G. P. 2013. Biological diversity mapping comes of age. Remote Sensing 5:374–376.

Asner, G. P., C. Anderson, R. E. Martin, D. E. Knapp, R. Tupayachi, F. Sinca, and Y. Malhi. 2014. Landscape-scale changes in forest structure and functional traits along an Andes-to-Amazon elevation gradient. Biogeosciences 11:843–856.

Asner, G. P., D. E. Knapp, J. Boardman, R. O. Green, T. Kennedy-Bowdoin, M. Eastwood, R. E. Martin, C. Anderson, and C. B. Field. 2012. Carnegie Airborne Observatory-2: Increasing science data dimensionality via high-fidelity multi-sensor fusion. Remote Sensing of Environment 124:454–465.

Asner, G. P., and R. E. Martin. 2009. Airborne spectranomics: mapping canopy chemical and taxonomic diversity in tropical forests. Frontiers in Ecology and the Environment 7:269–276.

Asner, G. P., and R. E. Martin. 2011. Canopy phylogenetic, chemical and spectral assembly in a lowland Amazon forest. New Phytologist 189:999–1012.

Baldeck, C., and G. Asner. 2013. Estimating vegetation beta diversity from airborne imaging spectroscopy and unsupervised clustering. Remote Sensing 5:2057–2071.

Beleites, C., and V. Sergo. 2012. hyperSpec: a package to handle hyperspectral data sets in R. R package version 0.98-20120923. http://hyperspec.r-forge.r-project.org

Bloom, S. A. 1981. Similarity indices in community studies: potential pitfalls. Marine Ecology Progress Series 5:125–128.

Bray, J. R., and J. T. Curtis. 1957. An ordination of the upland forest communities of Southern Wisconsin. Ecological Monographs 27:325–349.

Clark, M. L., D. A. Roberts, and D. B. Clark. 2005. Hyperspectral discrimination of tropical rain forest tree species at leaf to crown scales. Remote Sensing of Environment 96:375–398.

Gillespie, T. W., G. M. Foody, D. Rocchini, A. P. Giorgi, and S. Saatchi. 2008. Measuring and modelling biodiversity from space. Progress in Physical Geography 32:203–221.

Kreft, H., and W. Jetz. 2007. Global patterns and determinants of vascular plant diversity. Proceedings of the National Academy of Sciences USA 104:5925–5930.

Palmer, M. W., P. G. Earls, B. W. Hoagland, P. S. White, and T. Wohlgemuth. 2002. Quantitative tools for perfecting species lists. Environmetrics 13:121–137.

Rajaniemi, S., E. Tomppo, K. Ruokolainen, and H. Tuomisto. 2005. Estimating and mapping pteridophyte and Melastomataceae species richness in western Amazonian forests. International Journal of Remote Sensing 26:475–493.

Shannon, C. E. 1948. A mathematical theory of communication. Bell System Technical Journal 27:379–423.

Whittaker, R. H. 1960. Vegetation of the Siskiyou Mountains, Oregon and California. Ecological Monographs 30:279–338.

Supplemental Material

Appendix A

Field plot network description (*Ecological Archives* A024-077-A1).

Appendix B

Pseudo-code for mapping biodiversity using the spectral species distribution (*Ecological Archives* A024-077-A2).

Appendix C

Optimal component selection for biodiversity estimation using spectral species distribution (*Ecological Archives* A024-077-A3).

Appendix D

Extended comparison of methods developed for the estimation of α-diversity and based on the spectral variation hypothesis (*Ecological Archives* A024-077-A4).